

Near-infrared template spectra of normal galaxies: k-corrections, galaxy models and stellar populations.

F. Mannucci¹, F. Basile², B.M. Poggianti³, A. Cimatti⁴, E. Daddi²,
L. Pozzetti⁵, and L. Vanzi⁶

¹ *C.A.I.S.M.I. - C.N.R., Largo E. Fermi 5, I-50125, Firenze*

² *Università di Firenze, Largo E. Fermi 5, I-50125, Firenze*

³ *Osservatorio Astronomico di Padova, vicolo dell'osservatorio 5, I-35122 Padova*

⁴ *Osservatorio Astrofisico di Arcetri, Largo E. Fermi 5, I-50125, Firenze*

⁵ *Osservatorio Astronomico di Bologna, via Ranzani 1, I-40127, Bologna*

⁶ *European Southern Observatory, Alonso de Cordoba 3107, Santiago, Chile*

Submitted. Accepted

ABSTRACT

We have observed 28 local galaxies in the wavelength range between 1 and 2.4 μm in order to define template spectra of the normal galaxies along the Hubble sequence. Five galaxies per morphological type were observed in most cases, and the resulting RMS spread of the normalized spectra of each class, including both intrinsic differences and observational uncertainties, is about 1% in K, 2% in H and 3% in J. Many absorption features can be accurately measured. The target galaxies and the spectroscopic aperture ($7'' \times 53''$) were chosen to be similar to those used by Kinney et al. (1996) to define template UV and optical spectra. The two data sets are matched in order to build representative spectra between 0.1 and 2.4 μm . The continuum shape of the optical spectra and the relative normalization of the near-IR ones were set to fit the average effective colours of the galaxies of the various Hubble classes. The resulting spectra are used to compute the k-corrections of the normal galaxies in the near-IR bands and to check the predictions of various spectral synthesis models: while the shape of the continuum is generally well predicted, large discrepancies are found in the absorption lines. Among the other possible applications, here we also show how these spectra can be used to place constraints on the dominant stellar population in local galaxies. Spectra and k-corrections are publicly available and can be downloaded from the web site <http://www.arcetri.astro.it/~filippo/spectra>.

Key words: galaxies: elliptical and lenticular, cD - galaxies: photometry - galaxies: spiral - galaxies: evolution - galaxies: stellar content - infrared: galaxies.

1 INTRODUCTION

Galaxies are complex systems where gas, dust, stars and dark matter deeply interact with each other for a very long time. The emerging spectrum is therefore sensitive to a number of parameters as mass, age, metallicity, star formation history, dust, geometry etc. Despite this complexity, many groups have tried to model the galaxy emission, and the observed optical spectra can now be accurately reproduced (e.g. Bruzual & Charlot, 1993; Worthey, 1994; Fioc & Rocca-Volmerange, 1997; Barbaro & Poggianti, 1997; Tantalo et al., 1996). This is increasingly important as more high-redshift galaxies are discovered and important quantities as age, mass and star formation history are estimated

by comparing the integrated properties of the galaxies with the predictions of spectrophotometric models.

These models are calibrated on local galaxies and the first test on their properties is the comparison of the modeled spectra with the observed ones over a large wavelength range. Until now, this comparison could only be done in the optical and near-UV region where representative galaxy spectra are available (e.g., Pence, 1976; Coleman, Wu & Weedman, 1980; Kennicutt, 1992a, 1992b; Kinney et al., 1996, hereafter K96), while photometric points are used for all the other wavelengths. The aim of this work is to extend the range where a full comparison is possible towards longer wavelengths, between 1 and 2.4 μm . This is in particular important because large differences are present between the

different models especially in this wavelength range where the relative contribution of dwarf, giant and supergiant stars is poorly known (e.g., Charlot, Worthey & Bressan 1996). These stellar populations are characterized both by different depths of the absorption lines and different shapes of the near-IR continuum (see, for example, Pickles, 1998; Lançon et al., 1999) and therefore by studying breaks, colours and lines of a full spectrum it is possible, in principle, to separate their contribution.

Near-IR spectra can also be used to compute the k-corrections of an unevolving galaxy population, and, therefore, to study the luminosity functions and the differential evolution of the galaxies (Pence, 1976; Coleman et al. 1980, Frei & Gunn 1994, Poggianti, 1997). The near-IR k-corrections are becoming more and more important as new IR-optimized telescopes are becoming available, as the Very Large Telescope, the Large Binocular Telescope and the Next Generation Space Telescope. Complete spectra between UV and near-IR wavelength can also play a role in the measure of the redshifts of large samples of galaxies, both from photometric data (for a review see Yee 1998) and even from spectroscopic data (eg., Glazebrook, Offer and Deeley, 1998).

In this paper we show the results of the observations of 28 galaxies of morphological type between E and Sc, while later classes will be the subject of a future work. Target selection, observations and data reduction are described in sec. 2. Great care was taken in matching the near-IR spectra to the optical ones by using the observed UV-optical-IR colours, as described in sec. 3 and sec. 4. In sec. 5 we derive the k-corrections in the J, H and K band. In the following sections, we compare the total spectra to the predictions of some spectrophotometric models for elliptical galaxies and use the observed absorption lines to study the dominant stellar populations. Spectra and k-corrections are available in electronic form.

2 OBSERVATIONS AND DATA REDUCTION

The target galaxies were selected in the morphological classes E, S0, Sa, Sb and Sc. In each class we selected large nearby galaxies without indication for peculiar activity. An absolute magnitude threshold of $M_V < -21$ was used to ensure a homogeneous metallicity and to allow a sample as close as possible to that in K96. We also mainly observed galaxies whose optical spectra were available in the literature to be also able to study single objects. Therefore we selected galaxies from the samples by K96 and Kennicutt (1992a, 1992b), adding one more elliptical galaxy from the list given in Goudfrooij (1994). The resulting 28 targets are listed in Table 1, together with the morphological informations derived either from the LEDA catalog (<http://leda.univ-lyon1.fr/leda/>) or from the reference listed in the table. The objects are sorted in the table and divided into 5 classes according to the morphological index T (see, for example, Buta et al., 1994).

We planned to have 5 galaxies for each class between E and Sc with good S/N ratio (SNR) to have an estimate of the intrinsic spread in the spectra of each class and to average out peculiar characteristics. This number was not reached for the Sa class because NGC2798 turned out to

Table 1. Observed galaxies

NGC	R.A. (1950)	DEC.	Type	T ^a	Ref. ^b	Bands ^c
E ($-5 \leq T < -3$)						
4648	12:39:54.5	+74:41:44	E3	-4.9	1	JHK
1700	04:54:28.1	-04:56:30	E4	-4.8	2	JHK
3379	10:45:11.3	+12:50:48	E2	-4.8	1	JHK
4472	12:27:13.9	+08:16:22	E1	-4.7	1	JHK
4889	12:57:43.7	+28:14:54	E4	-4.3	1	JHK
S0 ($-3 \leq T < 0$)						
1023	02:37:15.5	+38:50:56	E-S0	-2.6	3	JHK
3245	10:24:30.1	+28:45:45	S0	-2.1	1	JHK
4350	12:21:25.1	+16:58:21	S0	-1.8	3	JHK
4382	12:22:52.8	+18:27:59	S0-a	-1.3	3	JHK
5866	15:05:07.0	+55:57:20	S0-a	-1.3	1	JHK
Sa ($0 \leq T < 2$)						
2681	08:49:58.0	+51:30:14	S0-a	0.4	3	JHK
3623	11:16:18.6	+13:22:00	SBa	1.0	1	JHK
2775	09:07:41.0	+07:14:35	Sab	1.7	1	JHK
3368	10:44:06.9	+12:05:05	SBab	1.7	1	JHK
Sb ($2 \leq T < 4$)						
4826	12:54:16.9	+21:57:18	Sab	2.4	3	JHK
4736	12:48:31.9	+41:23:32	Sb	2.5	3	JHK
2841	09:18:34.9	+51:11:19	Sb	3.0	3	HK
4102	12:03:51.6	+52:59:23	SBb	3.1	3	JHK
3147	10:12:39.3	+73:39:02	Sbc	3.7	1	JH
Sc ($4 \leq T < 6$)						
2903	09:29:20.2	+21:43:19	SBbc	4.0	1	JHK
5194	13:27:45.9	+47:27:12	Sbc	4.1	3	JHK
3994	11:55:02.3	+32:33:23	Sc	4.9	3	JHK
1637	04:38:57.5	-02:57:11	Sc	5.0	3	HK
2276	07:10:22.0	+85:50:58	Sc	5.4	1	K
Others						
3432	10:49:42.9	+36:53:09	Irr	9.0	3	
2798	09:14:09.4	+42:12:34	Sap	1.7	1	
1569	04:26:05.8	+64:44:18	Irr	8.2	1	
4449	12:25:45.9	+44:22:16	Irr	9.3	1	

^a: morphology stage index (e.g., Buta et al., 1994)

^b: references. 1: Kennicutt (1992b); 2: Goudfroij (1994); 3: K96.

^c: bands used for the templates

be peculiar (it is part of an interacting system) and with emission lines. This galaxy is listed in the ‘‘Others’’ section of Table 1 together with 3 more observed objects of later stages not used for the templates.

All the spectra were obtained at TIRGO, an IR-optimized 1.5m telescope on the Swiss Alps. We used the long-slit spectrometer LonGSp (Vanzi et al., 1997b) which is based on a NICMOS3 256×256 pixels Rockwell array and is sensitive between 0.9 and 2.5 μ m.

Each galaxy was observed through the largest available slit, 7'' wide, in order to have a good coverage of the galaxy. Spectra were obtained in the J, H and K bands for integration times between 15 and 30 minutes for each band. The resulting spectral resolution is about 300 in J, 400 in H and 500 in K. The telescope was chopped every minute

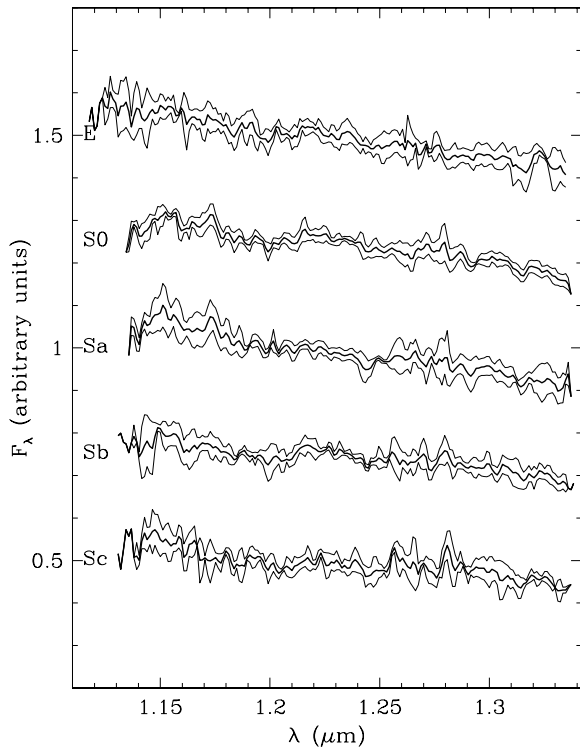


Figure 1. Rest frame average spectra of each class of galaxies in the J band. The thick line is the average of the observed spectra, the thin lines show the ranges within 1 standard deviation. Arbitrary offsets were added to the spectra for clarity.

between the galaxy and the nearby sky to have a good sky subtraction. Each time the galaxy was placed on a different position of the slit to minimize the effect of bad pixels and distortions of the flat-field. For each galaxy, stars of spectral type between F8 and G8 were observed in order to measure the atmospheric transmission and the variation of the instrumental efficiency with the wavelength, as discussed in Maiolino & Rieke (1996). The total number of acquired images is about 7000.

All the spectra were sky subtracted using the average of the adjacent spectra, and divided by differential flat-fields obtained by imaging the dome. The resulting frames were then rectified, co-aligned and stacked together using a clipping algorithm. A one-dimensional spectrum was then extracted from the central $53''$ in order to maximize the observed fraction of the galaxies. The resulting aperture of $7'' \times 53''$ is similar to the aperture of $10'' \times 20''$ used by K96 to define their templates and allows us to merge the two data sets. At the average distance of the galaxies of our sample, $27h_{50}^{-1}$ Mpc ($h_{50} = H_0/50$ km/sec/Mpc), the spectroscopic aperture corresponds to about 1×7 Kpc. We estimated the fraction of the galaxy light collected by the slit by using the existing aperture photometry in the V band (Prugniel and Héraudeau, 1998): on average, our spectra contain about 20% of the galaxy light, ranging from 7% for the closest and largest galaxies to about 35% for the smallest ones. Therefore our results should not be considered “total” spectra, even if the difference is expected to be negligible in the near-

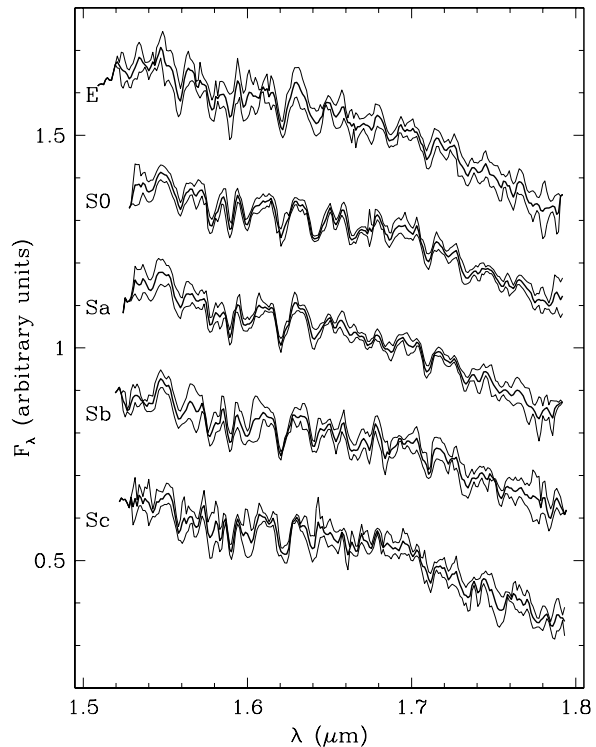


Figure 2. As Figure 1, H band

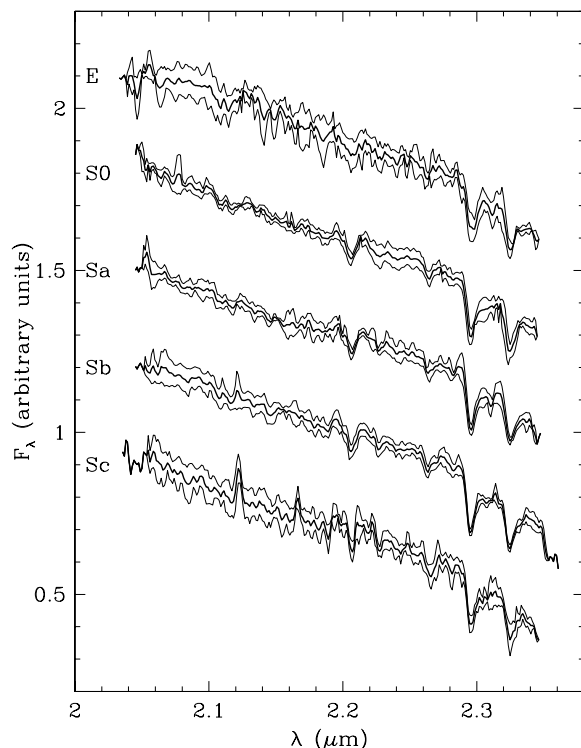


Figure 3. As Figure 1, K band

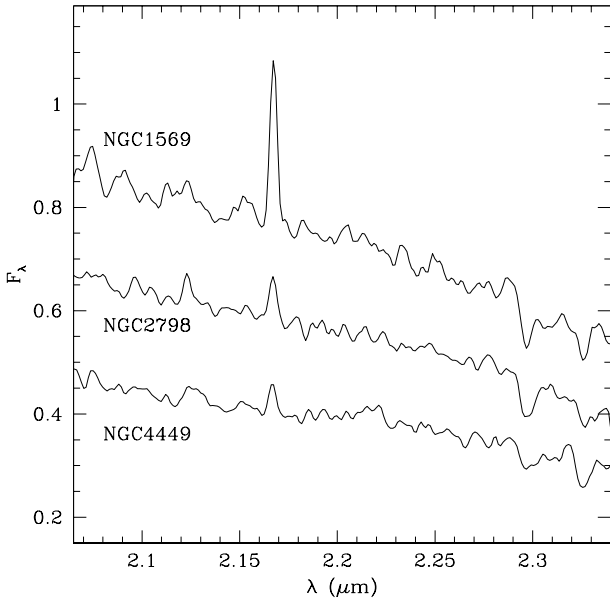


Figure 4. K-band spectra of the galaxies with active star formation NGC1569, NGC2798 and NGC4449, The emission lines at $2.122\mu\text{m}$ (H_2) and 2.166 ($\text{Br}\gamma$) can be seen in the spectra.

IR (see discussion below). This is more important when also the K96 spectra are considered as in the optical the radial gradients are expected to be larger (but see also the discussion in K96).

The “true” spectra of the reference stars were modeled by the solar spectrum (Livingston & Wallace, 1991) corrected for the slightly different temperature of the stars. The derived transmission curve was then applied to the galaxy spectra. The final spectrum of each galaxy in each band is then corrected for Galactic extinction, normalized, shifted to zero redshift, and averaged with the other galaxies of the same class. A clipping algorithm was applied to remove a few residual discrepant value due to cosmic rays, erratic bad pixels not present in the mask and uncorrected features of the reference stars. In Figures 1,2 and 3 we show the average spectra and the relative standard deviations in the three bands.

The differences between the spectra of the galaxies of the same class is due to both all the observational uncertainties (noise, residual sky contribution, distortion on the flat field, non perfect correction of the instrumental and atmospheric transmission) and the intrinsic differences between the observed galaxies. We can therefore have a robust upper limit of the total uncertainties of our spectra by looking at the resulting RMS among the galaxies of the same type. This quantity is between 0.7% and 1.4% in K, between 1.7% and 2.4% in H and between 2.4% and 3.6% in J, depending on the morphological class. The tendency to have larger spreads towards bluer wavelengths is probably dominated by larger intrinsic differences, and the value in K, about 1%, can be assumed as the real uncertainty in the single spectrum. Because of the different redshift of the galaxies, less galaxies contribute to the edges of the spectra and therefore the un-

certainties tend to be larger in the external part (about 5%) of the bands. The parts of the spectra without indication of standard deviation in figures 1,2 and 3 have been derived from only a galaxy and should be treated with caution.

If the normal galaxies show a high degree of uniformity, on the contrary large differences are found for the few galaxies with peculiar properties or of later types. The K spectra of 3 of these galaxies (NGC1569, NGC2798 and NGC4449) are shown in Figure 4, while for NGC3432 the SNR is too low. The galaxies in the figure show prominent emission lines whose brightness and ratios change much from one object to the other. In this case no attempt was made to create a template.

3 CALIBRATION OF THE SPECTRA

We now want to establish the relative calibration of the spectra in the various bands to be able to study the overall spectral energy distribution from the UV to the near-IR. It is not possible to derive these relative normalizations by simply using spectral observations because of several effects, such as slit losses, variability of the atmospheric transmission and uncertainties on the reference star colours. The usual method to normalize spectra taken in different bands is to use the broad-band colours of the target objects: spectra should be calibrated to reproduce the colours of the observed galaxies inside the spectroscopic aperture.

As this work is aimed at the construction of spectra representative of the average properties of the different classes of galaxies, we have calibrated the spectra by using the average colours of each class. This method guarantees that the final spectra closely match the average properties of the class and allows the reduction of the uncertainties on the colours as hundreds of galaxies can be used.

Of course, colours inside our rectangular spectroscopic aperture are not available. However, the dependence of near-IR colours and spectra with aperture is known to be very weak because the dominant stellar population at these wavelength is always the giant branch (with the exception of starburst galaxies, see for example, Maraston (1998)) and only the second-order metallicity and age gradients could be seen. Therefore we can use colours inside circular apertures as they are the only ones usually published, and the difference in shape between photometric and spectroscopic apertures is negligible if the two areas are chosen to be similar. The most similar circular aperture with enough published photometric data is the “effective” one, i.e., the aperture containing half of the light of the galaxy in the B band. Effective colours are available for a large number of galaxies and in many filters and is therefore possible to have large homogeneous data sets.

For the smallest objects, the effective aperture is similar to the spectroscopic one, for the largest galaxies the photometric aperture is larger. We have performed two checks to be sure that, even in the latter case, effective colours can reliably be used to calibrate the spectra: first we have compared spectra extracted from the central $10''$ of the slit with those of the outer part; second, we have compared the spectra of large and small galaxies of the same class (as NGC4350 having $D_0=2'.0$ and NGC4382 with $D_0=8'.2$). In both cases no systematic differences are seen.

Table 2. Average effective colours of galaxies with $M_V < -21$. For each colour the standard deviation and the number of used objects are also reported.

	U-B	B-V	V-R	V-I	V-K	J-H ^a	H-K ^a
E	0.50 (0.08) 323	0.99 (0.05) 418	0.59 (0.05) 314	1.22 (0.07) 221	3.30 (0.09) 32	0.66 (0.05) 225	0.21 (0.02) 225
S0	0.47 (0.11) 287	0.97 (0.08) 344	0.58 (0.05) 227	1.20 (0.08) 158	3.25 (0.14) 13	0.66 (0.05) 235	0.22 (0.02) 235
Sa	0.36 (0.19) 138	0.90 (0.11) 185	0.58 (0.08) 73	1.17 (0.11) 82	3.24 (0.18) 17	0.67 (0.06) 105	0.25 (0.03) 105
Sb	0.22 (0.20) 321	0.82 (0.12) 541	0.57 (0.09) 156	1.16 (0.11) 315	3.21 (0.28) 16	0.66 (0.06) 93	0.25 (0.03) 93
Sc	0.06 (0.18) 294	0.70 (0.13) 536	0.52 (0.10) 133	1.15 (0.15) 287	3.03 (0.24) 23	0.66 (0.07) 46	0.25 (0.04) 46
Sd ^b	-0.12 (0.16) 53	0.62 (0.18) 99	0.47 (0.13) 25	1.09 (0.19) 58	2.95 (0.32) 12	0.65 (0.08) 26	0.23 (0.05) 24
I ^c	-0.15 (0.20) 102	0.51 (0.17) 117	0.40 (0.20) 28	1.08 (0.30) 35	2.35 (0.35) 5	0.51 (0.10) 22	0.21 (0.06) 20

^a: The J-H and H-K colours are based also on the results in Fioc & Rocca-Volmerange, 1999, where only average quantities are given. In these cases the scatter is not measured but estimated.

^b: $M_V < -20$

^c: no magnitude selection.

Once the aperture is chosen, we have also to select the luminosity of the galaxies used to derive average colours. As described in the previous section, the target objects are large, metal rich galaxies, and we want to use galaxies with the same properties to calibrate their spectra. In fact, smaller galaxies tend to be less metallic and therefore bluer in the optical colours (see, e.g., Fioc & Rocca-Volmerange, 1999), giving origin to the well-known colour-magnitude relation. We will use optical and near-IR colours appropriate for galaxies with $M_V < -21$, corresponding to our sample.

Many photometry papers where used to derive these colours and check the results (Aaronson, 1978; Frogel et al., 1978; Persson et al., 1979; Griensmith et al., 1982; Glass, 1984; Giovanardi & Hunt, 1988; de Jong & van der Kruit, 1984; de Vaucouleurs et al., 1991; Buta et al., 1994, 1995a, 1995b; Prugniel & Héraudeau, 1998; Fioc & Rocca-Volmerange, 1999). The optical colours are mainly based on the Prugniel & Héraudeau (1998) catalog after correcting for Galactic dust using the RC3 value of the galactic extinction in B (de Vaucouleurs et al., 1991) and the Cardelli et al. (1989) extinction curve. The E and S0 optical-to-IR colours are based on Persson et al. (1979) and Frogel et al. (1978), while the colours of later spirals are mainly derived from Griensmith et al. (1982), de Jong & van der Kruit (1984)

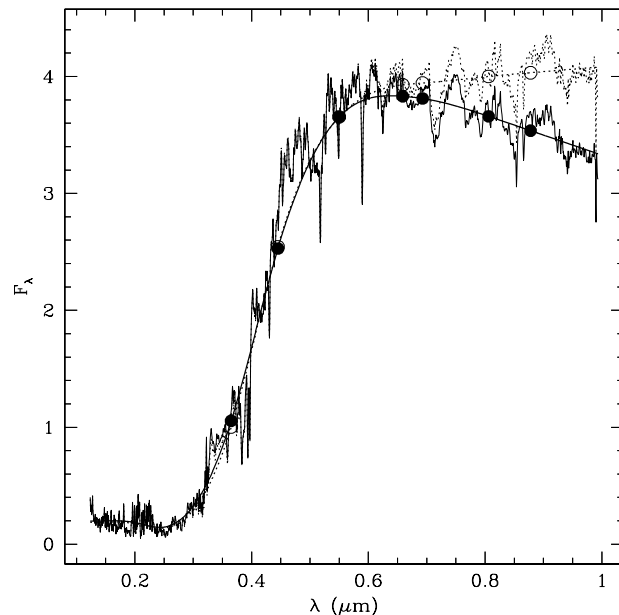


Figure 5. Colour correction to the K96 spectra. The dotted lines show the K96 spectrum for the ellipticals and a spline fit to the corresponding photometric points. (empty dots). The solid dots show the effective colours of the galaxies of this class with $M_V < -21$ (see Table 2), the solid lines are the fit to these data and the final spectrum, corrected to fit the colours.

and Aaronson (1978). IR-to-IR colours are based on Glass (1984), Frogel et al. (1978) and Fioc & Rocca-Volmerange (1999). Note that the J-H and H-K colours of the early-spiral galaxies are redder than those of the ellipticals: a short discussion about this unexpected effect can be found in Fioc & Rocca-Volmerange (1999). All the colours were converted to Johnson's U, B and V, Cousins' R and I and CIT J, H and K. Great care was used in comparing different galaxy samples: whenever possible, the results from different galaxy samples were compared to each other to check for consistency and to discover any important selection effect. The results are listed in Table 2 together with the colour scatter and the number of galaxies used. The absolute magnitude threshold was reduced to $M_V = -20$ for the Sd class ($6 < T < 8$) because these galaxies are on average intrinsically fainter than the other classes, and for the I class ($T > 8$) no magnitude restriction was used because of the large scatter observed. The colours of these latter two classes (not used for the templates and reported for completeness) are based on a smaller number of galaxies and are probably less accurate than the others.

Earlier classes tend to be more homogeneous than the later ones. For the ellipticals, the spread of the colour distribution, when removing a few very discrepant objects, is comparable to the uncertainties on the single measure as quoted in the original papers, leaving little room to an intrinsic spread of the population due, for example, to different metallicity or star formation histories. On the contrary, for the later class the observed spread is several times larger than the measured uncertainties. As an example, for the ellipticals the V-K colour distribution has a standard deviation of 0.09 mag (and an error on the mean of the order

of 1%), similar to the average estimated error on the single point of about 0.10 mag, while for Sc the observed spread is 0.24 mag.

4 MATCHING OPTICAL AND NEAR-IR SPECTRA

The same colour calibration was used to match our spectra to existing optical and UV ones to obtain a single template from 0.1 to 2.4 μm . Several optical templates are available in the literature (Coleman et al., 1980; Kennicutt, 1992a, 1992b; K96). In order to obtain meaningful results, the optical spectra must have appropriate resolution and wavelength coverage, should be based on a relatively large number of galaxies and the used spectroscopic aperture must be similar to our one. Among the available optical templates, only the K96 spectra have the required features: 1- they have a high enough resolution (between 6 and 10 \AA) for most studies of stellar populations; 2- have the largest wavelength coverage, extending from 1200 \AA up to about 1 μm , at the edge of the J band (the Sc spectrum covers only up to 7700 \AA); 3- use an aperture of 10 \times 20'' at all the wavelengths, similar to ours. 4- are based on the observations of 30 galaxies, 12 of which in common to our sample.

While below 7000 \AA the K96 spectra closely reproduce the observed colours of Table 2, above this wavelength the K96 spectra are much redder. The difference is not due to the chosen colours (effective aperture and $M_V < -21$) because the K96 spectra don't fit the average colours inside any aperture and for any magnitude (see, for example, Goudfrooij, 1994). Moreover, they don't reproduce the colours of the observed galaxies: as an example, all 4 elliptical galaxies in K96 have observed Johnson's V-I colours between 1.38 and 1.45 for apertures between 10 and 20'' (Prugniel & H eraudeau, 1998), while the colour derived from the K96 spectrum is 1.59. It should also be noted that above 7000 \AA the K96 spectra are quite different from those by Coleman et al. (1980) who also corrected the spectra for the observed colours. No useful comparison can be done with the Kennicutt (1992a, 1992b) atlas because it only covers the spectra region below 7000 \AA .

In order to have a self-consistent template we have to apply some corrections to the optical spectra to make them fit the colours. The procedure is shown in Fig. 5 where the K96 spectrum for the ellipticals is plotted against the colours of Table 2 used both to calibrate the near-IR spectra and to correct the K96 templates. The correction to the K96 spectra was computed by the ratio of two splines, fitted respectively to the observed colours and to the colours derived from the spectra (see Figure 5). This correction is not unique, but the availability of data in many filters maintains this uncertainty below the other ones.

For all the K96 spectra between E and Sb, a good agreement (within a few percent) is present below 7000 \AA between the optical spectra and the average colours, and the corrections are small. On the contrary, the Sc spectrum, based on two galaxies only, appears to be much bluer than the expected colours of its class even at $\lambda < 7000 \text{\AA}$. Also the equivalent widths of the emission lines are much larger than in the galaxies of our sample, about 296 \AA for the $H\alpha + [\text{NII}]$ vs. an average of 41 \AA for our galaxies (Kennicutt & Kent,

1983) and 54 \AA for the Sc sample by Kennicutt (1992a). We think that both these effects are probably due to the fact that the two Sc galaxies in the K96 sample, NGC 598 and NGC 2403, are of later type ($T=5.6$ and 5.7) than the average Sc ($T=5.0$, from Buta et al., 1994) and those in our sample ($T=4.7$). To correct for this, we have both applied the colour correction, as for the other types, and also scaled down the emission line to have the same EW of our sample. The resulting spectrum, although representative of an average Sc galaxy, should be used with caution when comparing optical to near-IR features and when dealing with the emission lines, also because of its lower SNR.

As final step, the spectra were arbitrarily interpolated across the wavelength ranges where the atmosphere is not transparent. In Figure 6 we show at a reduced resolution the final spectra reproducing the observed effective colours.

The relatively small apertures used for both spectroscopy and photometry means that the spectra in Figure 6 are representative of the central regions of the galaxies containing about half of the total emission. K96 compare their optical spectra with those by Kennicutt (1992b) obtained using a much larger aperture (about 90 \times 90'') and conclude that for E, S0 and Sa the K96 spectra are in fact representative of the total emission of the galaxies because their integrated properties are dominated by the central bulge. The same argument applies in the near-IR too, and in this case a weaker dependence of the spectra from the aperture is also predicted: in fact, while in the optical the young population in the upper main sequence can easily dominate, in the near-IR any shortly living super-giants population must compete with the usually much more numerous giants population and therefore dominates only in case of strong activity of star formation. As discussed in the sec. 3, this can be checked comparing near-IR spectra extracted from the inner and outer regions of the galaxies, or from large and small objects. A weaker variation of the near-IR spectra with aperture with respect to the optical spectra can also be predicted from the colours: the J-H and H-K colours are only weakly dependent of the galaxy type (see Table 2) and do not show significant radial gradients (Glass 1984; Fioc & Rocca-Volmerange, 1999), not even for the late type galaxies. Therefore we conclude that for the early type galaxies the spectra in Figure 6 can also be used as templates of the integrated galaxy. For Sb and Sc galaxy, younger extra nuclear populations can change the spectra significantly, both in the optical because of the stars of the upper main sequence and in the near-IR if an important population of red supergiants is present.

5 THE K-CORRECTIONS

The first quantities that can be derived from these spectra are k-corrections, i.e., how magnitudes and colours change with the redshift because of the shift of the observed wavelength ranges. These corrections are crucial to link the properties of the local universe with the distant one (see, for example, Peebles, 1993), and their accurate knowledge is important to study the evolutionary effects. Our spectra allow us to compute these corrections in the near-IR filters starting from $z=0$ with a greater accuracy than by using simple broad-band photometry as, for example, Cowie et al. (1994).

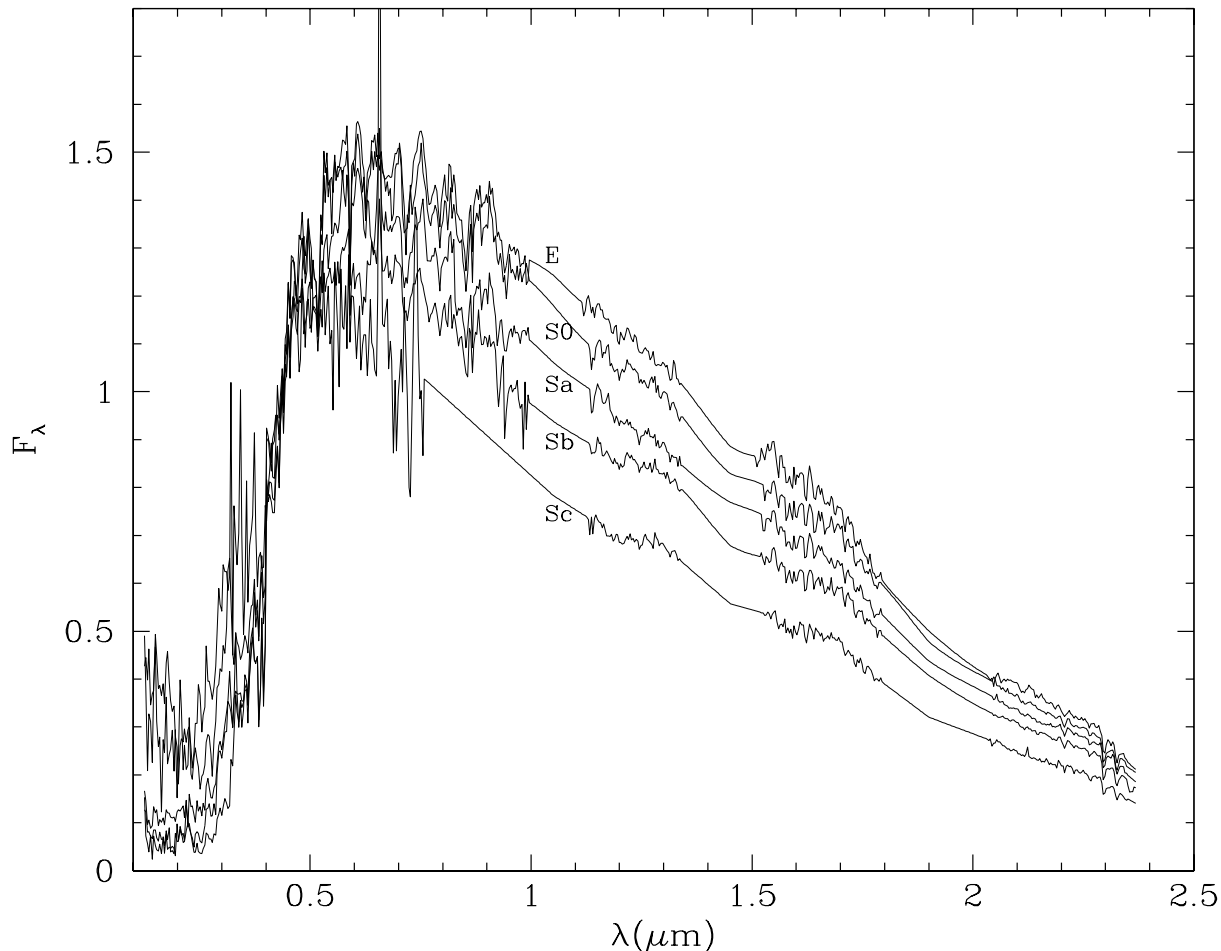


Figure 6. Template spectra for E, S0, Sa, Sb and Sc galaxies. The spectra were reduced to a resolution of 40\AA and normalized to the B band. The interpolation between the bands is arbitrary.

In Figure 7 we show the k-corrections computed for the J, H and K bands. These filters have an increasing importance in the surveys for distant galaxies and in the study of the known high-redshift objects, especially when more 8-meters class space- and ground-based telescopes optimized for the infrared will be available.

The k-corrections were computed using Bessell & Brett (1988) filters, more standard than the CIT system. We note that in the K band the k-corrections are almost independent from the galaxy type up to $z=2$, reflecting the dominance of giant stars in these wavelengths in all the observed galaxies, as previously noted (Glazebrook et al. 1995). Note that no contributions are included from galaxy evolution or increasing absorption from the intergalactic medium; the computation is limited to $z=2$ because above this limit these effects are certainly dominant.

We have compared our k-correction in the K band with others previously published. At low redshift ($z < 0.6$) we found consistency with the k-correction by Glazebrook et al. (1995) derived from Bruzual & Charlot (1993) model for a SSP with age of 5 Gyrs, and used, for example, by Loveday (2000) and Szokoly et al. (1998) to define the local luminos-

ity function. On the contrary, big differences (up to 0.2 mag) are found with k-correction from ‘UV-hot’ elliptical model of Rocca-Volmerange & Guiderdoni (1988). At higher redshift ($z > 0.6$) our k-corrections are ‘redder’ up to 0.3 magnitudes than previous ones, however at these redshifts they should be taken with caution, and considered as lower limits, due to the possible evolutionary effect on galaxy spectrum.

Important differences are also found with the k-corrections by Poggianti (1997). Regarding the SED of the elliptical, the difference in J is generally about 0.1 and in H is always below 0.2, while differences greater than 0.3 are found in the K band in the redshift range $z=0.3$ to 1.3, up to a value of about 0.45 magnitudes at $z=0.4-0.7$. Although the differences in the filter response functions adopted here and in Poggianti (1997) contribute to the differences between the K-corrections, most of the K-band discrepancy arises from intrinsic differences in the SED, probably due to the sparse sampling of the Poggianti (1997) models at $\lambda > 17000\text{\AA}$. The comparison for Sa and Sc galaxies is less meaningful because of large spectral variations within each morphological class, possible aperture effects (see §4), especially for Sc

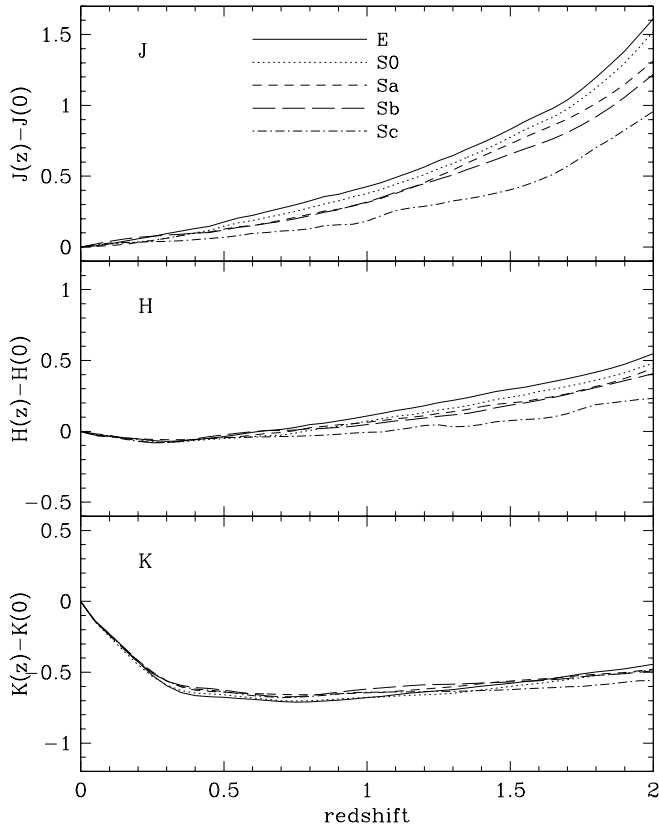


Figure 7. k-corrections in the J, H and K bands between redshifts 0 and 2 for each morphological type: E (solid line), S0 (dotted), Sa (short dashed), Sb (long dashed) and Sc (dot-dashed). Our spectra define these k-corrections up to $z=0.3$ in J, $z=0.7$ in H and 1.2 in K, while at higher redshift they reflect the K96 spectra corrected to match the observed colours.

galaxies, and the presence of emission lines, not included in the Poggianti (1997) model.

6 COMPARING OBSERVATIONS AND MODELS

Template spectra can be used to test the spectrophotometric models of the galaxies. Despite their low resolution, the SNR is high enough to allow useful comparison of both the continuum shape and the spectral features. Here we show two examples of the possible use of these spectra. The first one, described in this section, is the comparison of the shape of the continuum over a large wavelength range. In the next section the absorption lines will be compared.

Two reasons suggest to start the continuum comparison from the elliptical galaxies: first, from the observational point of view this class is the most homogeneous, its average colours are better defined and the spectrum has smaller uncertainties. Second, elliptical galaxies are known to be dominated by old stellar populations and therefore the uncertainties on the star formation history (SFH) have lower consequences than in the case of the spirals: while in the

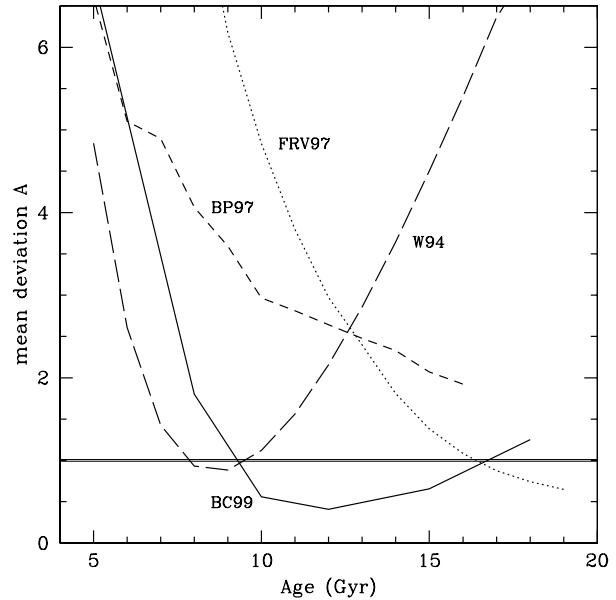


Figure 8. Mean deviation of the predictions of some spectrophotometric models from the observed spectrum of the elliptical galaxies as a function of the age of the stellar population. Details about the models can be found in the text.

latter case detailed SFH are required to fit the spectra, for the ellipticals a single parameter, the age, is usually enough to obtain a good agreement.

We used four different models: the Bruzual & Charlot model in the 1999 version (BC99), the Fioc & Rocca-Volmerange (1997) PEGASE model (FRV97) the Barbaro & Poggianti (1997) one (BP97), and the model by Worthey (1994) (W94). We have also used a previous (1996) version of the Bruzual & Charlot model (BC96) that allows for non-solar metallicities.

BC99 and BC96 use isochrones from the Padova group (Bressan et al., 1993) and two different stellar libraries, the empirical library from Pickles (1999) and the theoretical one by Lejeune et al. (1997). The latter library permits to predict the spectra of galaxies of various metallicities, from 5% to 250% solar. BC99 and BC96 give the spectra of an instantaneous burst of star formation (the so called Simple Stellar Population, SSP) that can be integrated over the time to reproduce an arbitrary SFH. We used a Salpeter Initial Mass Function (IMF) between 0.1 and $125 M_{\odot}$. The BC96 model was used mainly because it allows to use non solar metallicities.

The FRV97 models use a different approach: starting from some hypothesis on the efficiency of the star formation processes, they model the entire life of the galaxy in order to reproduce the observed spectrum. The resulting SFH for ellipticals is a rapidly declining exponential law giving most of the star formation in the first Gyr, while for the Sc the SFH is almost constant over an Hubble time. The chemical evolution is also computed, but is not used for the final spectrum which assumes solar metallicity. The Padova isochrones are used, together with the empirical stellar library by Gunn &

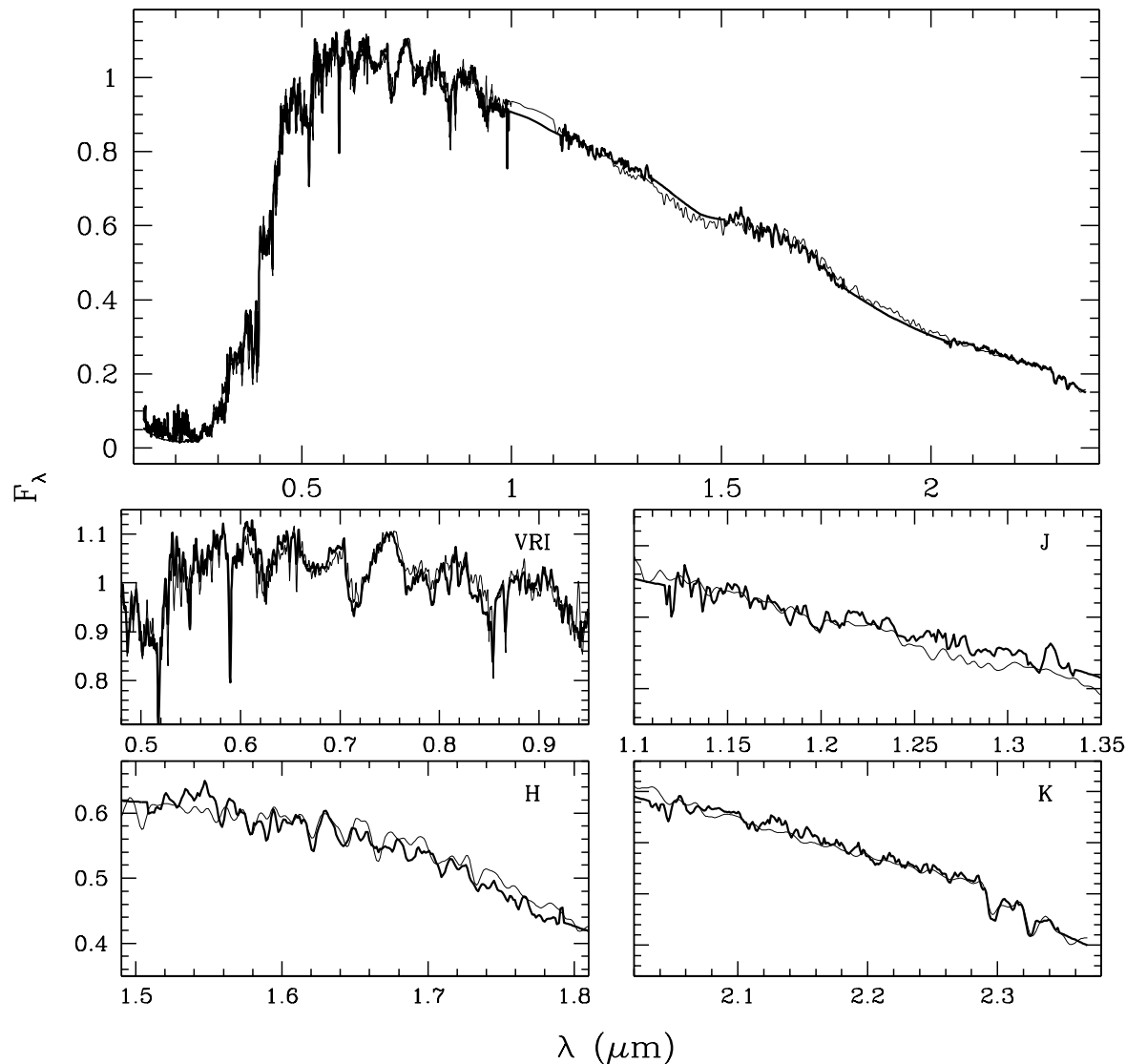


Figure 9. The observed spectrum of the elliptical galaxies (thick line) is compared with a SSP spectrum of the BC99 model (thin line) with an age of 12 Gyr and solar metallicity. The upper panel shows the full spectrum, the four lower panels show enlargements in the optical and in the three near-IR bands. The shape of the spectrum is very well reproduced in all the range between 0.2 and 2.4 μm , and this is true for the optical absorption features too. In the near-IR large discrepancies can be noted, especially in J and H. The reason of these differences are explained in the text.

Stryker (1983) and Lançon & Rocca-Volmerange (1992) and the IMF by Rana (1992).

The BP97 model has the same approach of BC96, computing the galaxy integrated spectrum adding up the contribution of SSPs of (possibly) different metallicities. It uses the Padova isochrones and the Salpeter IMF between 0.1 and 100 M_{\odot} . The stellar spectra in the optical are either from Kurucz (1993) or from Jacoby et al. (1994), while the library by Lançon & Rocca-Volmerange (1996) are used in the near-IR. In this paper we only consider BP97 spectra

up to 1.8 μm because above this limit the Kurucz sampling becomes too sparse.

The W94 model provides with single-age stellar population with metallicities between 0.01 and 3 times solar. It uses stellar evolution isochrones by Vandenberg and collaborators and by the Revised Yale Isochrones (Vandenberg & Laskarides, 1987; Green et al., 1987), Salpeter IMF and theoretical stellar spectra by Kurucz (1993) and Bessell et al. (1994). A particular emphasis was put in studying the variation with metallicity and age of several optical spectral features.

For demonstration purposes and to better study the intrinsic differences between the models, for BC99, BC96, W94 and BP97 we used SSP spectra of solar metallicity. For FRV we used both the models of elliptical galaxy they present, named E13 and E16, corresponding to two different cosmologies. In all the cases we searched for the best fitting spectrum by changing the age, the only remaining parameter, between 5 and 19 Gyr. All the spectra, both observed and modeled, were normalized to have the same total flux between 0.3 and 2.35 μm and reduced to the same resolution. The difference between comparing spectra to spectra and spectra to broad-band colours is important: both the absorption features and the continuum shape inside each band are taken into account and can dominate the results, especially when the agreement with the colours is good.

To measure the deviation it is not possible to use the standard χ^2 because the fitting points are not totally independent of each other as the normalization of each band is given by the colour calibration (see section 3). Therefore we need a way to compare the deviations both to the spectrum noise and to the colour uncertainties. To do this we compute the square deviation Δ^2 between observed (o_i) and model (m_i) spectra in each band:

$$\Delta^2 = \sum_{i=1}^N \frac{(o_i - m_i)^2}{N}$$

where N is the number of spectral points, and divide it for the square sum δ^2 of the various error contributions. The final value A we use as analog to χ^2 is the average of these ratios in the optical and in three IR bands:

$$A = \frac{1}{4} \left[\left(\frac{\Delta^2}{\delta^2} \right)_{Op} + \left(\frac{\Delta^2}{\delta^2} \right)_J + \left(\frac{\Delta^2}{\delta^2} \right)_H + \left(\frac{\Delta^2}{\delta^2} \right)_K \right]$$

which has a value of 1 if the deviations are only due to the errors in the observed spectra. The quantities δ^2 are difficult to estimate with precision: from the RMS spread of the spectra (see section 2) and the error on the mean of the colours in table 2, we obtain $\delta = 0.03$ in the optical, J and H and $\delta = 0.02$ in K.

In Figure 8 we show the resulting values of A as a function of the galaxy age for the four used models and solar metallicity. Even taking into account the uncertainties on δ , for all the models an age exists which well reproduce the data: BC99 shows the best accord for ages between 10 and 16 Gyr, W94 select younger ages, between 8 and 9 Gyr, FRV97 reaches the best agreement for older ages, above 16 Gyr. The deviation of the BP97 model is always above 1 but steadily reduces toward older ages, reaching a value of about 2 at 16 Gyr, the maximum age available for the model. It should be noted that BC99, BP97 and W94 are single-burst models with the same IMF and metallicity, therefore the difference between them are due to something outside the user control, as isochrones or stellar spectra. FRV97 is not a single burst model, about 92% of the stars are formed in the first Gyr (about 97% in the first 4 Gyr) but the SFR never reaches a null value; this probably explains at least part of the differences with the other models and the requirement of very old ages.

In Figure 9 we show the best fitting model, the BC99 spectrum for an SSP of 12 Gyr of age, solar metallicity and empirical star spectra. The overall shape of the spectrum is

very well reproduced: the largest difference are in the interpolated region between 1 and 1.1 μm where the model trace the position of the continuum while our interpolation an “effective” level taking into account the absorption lines. On the contrary, at a closed look it is possible to see that important discrepancies remains in the details of the absorption lines, both if theoretical and observed star spectra are used. This will be the subject of the next section.

We also tested the effect of changing the metallicity by using the BC96, W94 and BP97 models with metallicities 2.5 times solar, BC96 0.2 solar and W94 0.3 solar. In all cases no good fit can be reached for any age, as the values of A remain above 5. Models with super-solar metallicities are too red for $\lambda > 8000\text{\AA}$, even for young ages (limited to be higher than 5 Gyr): as an example, all these models predict fluxes in the H band between 10% and 20% higher than observed. Vice versa for sub-solar metallicities: the H band flux is under predicted of about 20%. These discrepancies might be an indication of the real metallicity of the elliptical galaxies, but it is more probably due to inadequacy of the non-solar stellar library or isochrones. It is beyond the purpose of this paper to solve this ambiguity.

7 THE ABSORPTION LINES

The use of our spectra to study the absorption line is hampered by the low resolution, both because faint lines are below the detection threshold and because many lines are blended together. Nevertheless, many features can be easily seen and measured with great accuracy, even if in some cases their identification may not be unique. For the following analysis we have only used the spectra in H and K because a series of facts make our J spectra less useful to study the features: they have the lowest resolution, their SNR is lower than that in the other bands, the features are intrinsically less prominent, and the star classification in this band is still in its infancy (see, for example, Wallace et al., 2000).

To further increase the SNR we decided to use the average of the spectra of E, S0 and Sa because they show no significant difference in the absorption lines, meaning that temperature, luminosity and metallicity of the dominant stellar populations are similar. We will indicate with ES the resulting average spectrum.

We identified the lines (see Table 3) by comparing the features in our spectra to those identified in the late type stars. The literature of reference is now rich enough (e.g., Origlia et al., 1993; Oliva et al., 1995, 1998; Meyer et al., 1998, hereafter M98; Kleinmann & Hall, 1986, hereafter KH86; Vanzi & Rieke 1997; Wallace et al., 1996, 1997) to make the identifications reliable, but the dominant contribution to some features due to blending of many lines is sometime uncertain. In these cases, the synthetic spectra constructed specifically for line identification in the H band by Origlia et al. (1993) were of particular help, while in the K band the high-resolution spectra by Wallace et al. (1996) were taken into particular account.

The first useful results can be derived by qualitatively comparing the H- and K-band parts of the ES spectrum to various stellar spectra libraries and to the results of the spectrophotometric models. This comparison is shown in Fig-

Table 3. Feature Identification

λ (μm)	Main contribution	Other species
1.529	OH	CN,TiI
1.540	OH	SiI
1.558	^{12}CO	OH
1.577	^{12}CO	MgI,FeI
1.589	SiI	OH
1.598	^{12}CO	SiI, ^{13}CO
1.606	OH	
1.619	^{12}CO	OH,CaI
1.640	^{12}CO	SiI,[FeII]
1.652	^{13}CO	OH
1.661	^{12}CO	OH
1.669	SiI	OH
1.672	AlI	HI, ^{12}CO
1.677	AlI	
1.689	OH	HI,CO
1.710	MgI	CO,OH
1.723	OH	SiI
1.733	SiI	HI
2.067	FeI	
2.072	FeI	
2.081	FeI	SiI
2.107	MgI	H ₂ O,SiI
2.117	AlI	H ₂ ,MgI,FeI
2.136	SiI	
2.146	MgI	NaI,SiI,CaII
2.166	Br γ	VI
2.173	ScI	FeI
2.179	TiI	SiI,FeI
2.189	SiI	TiI,FeI
2.208	NaI	ScI,TiI,VI,FeI,SI
2.226	FeI	ScI,TiI
2.239	FeI	ScI
2.248	FeI	VI,TiI
2.263	CaI	ScI,TiI,FeI,SI
2.281	MgI	CaI,FeI,SI,HF
2.294	^{12}CO	TiI
2.323	^{12}CO	
2.345	^{13}CO	

ures 10 and 11 where all the spectra were normalized to a fitted continuum and reduced to the same resolution of the observed data.

In panel (a) of Figure 10 a K5III star from M98 is overplotted to the data. The agreement is very close and basically all the features are well reproduced: as expected, cold giant stars dominate the emission at 1.6 μm and the observed spectra can be reproduced even with a single star spectrum. Analogous excellent agreement is obtained using spectra from the Wallance & Hinkle (1996) library (not shown) which are limited to a narrower wavelength range.

The following panel shows the spectrum of two stars, a K5III and a M0III, from the more recent stellar libraries by Pickles (1998), library used in several spectrophotometric models. The former star, the same as panel (a), shows a spectrum similar to our data, even if the agreement is not as accurate as for the KH86 spectrum. On the contrary, the M0III star shows a very different behavior, as also other stars of similar spectroscopic and luminosity class. These differences are not explained by the small temperature difference

between the K5 and M0 stars (about 160 °K, M98) and such a behavior is not seen in other libraries, as M98 or Wallance & Hinkle (1996). The differences are probably due to the use of several different sources in the derivation of the Pickles (1998) library. In particular Pickles bases the near-IR part of its spectral on the the Lançon & Rocca-Volmerange (1996) library because it covers a wide wavelength range, between 1.43 and 2.5 μm , with accurate flux calibration. Unfortunately, some features of the spectra of this library seem very variable from one spectral type to the next ones and very different from other libraries (as M98 and KH86) and from our spectra. Therefore they probably are observational artifacts. As a consequence, any spectrophotometric model based on this library will not be able to accurately reproduce the features in near-IR galaxy spectra. This is shown in the following (c) panel: here the observed spectrum is compared to the BC99 SSP galaxy model at the age of the best fit in Figure 8. This model is the only one in our sample having a resolution in the near-IR high enough to allow a meaningful comparison of the spectral features. Even if the general shape of the continuum is well reproduced, as shown in Figure 8, the agreement with the spectra features is generally poor: as an example, the deep absorption lines predicted by the models at 1.665 and 1.705 μm are not present in the observed data.

Same conclusions follow from the spectra in the K band shown in Figure 11: the K5III star from KH86 in panel (a) shows a very good agreement with the ES spectrum. Only the CO bands at 2.29 and 2.32 μm are deeper in the star spectrum than in the ES one, because of either metallicity effects, or the contribution of stars warmer than K5 or on the main sequence, or differences in the fitted continuum level above 2.28 μm . Analogous excellent agreement is obtained with the K5III star spectrum from the Wallance & Hinkle (1996) library (not shown).

In panel (b) and (c) the Pickles (1998) and BC99 spectra are shown: again, some features are not reproduced. For example, the prominent NaI feature at 2.21 μm is almost completely absent from the M0III star and from the model spectra. Also the CaI feature at 2.26 μm appears deeper in the observed data than in the model spectrum. Given that the general shape of the continuum is well reproduced by the model, (see the previous section) the problem must be in the used stellar library.

To summarize, libraries of stellar spectra exist which reproduce the observed galaxy spectra, while others show very different features. Spectrophotometric models based on the second set of spectra might not be able to reproduce the observed features. Our spectra will make it possible to tune the models, especially when new and more extended libraries of near-IR stellar spectra will be available (see, for example, Ivanov et al, 1999; Mouhcine & Lançon, 1999).

8 THE DOMINANT STELLAR POPULATION

As discussed in the previous section, indications on the dominant stellar population can be easily derived even by simply comparing the observed data with the stellar spectra. More quantitative results can be obtained by comparing the absorption lines.

Several authors have used this method to classify the

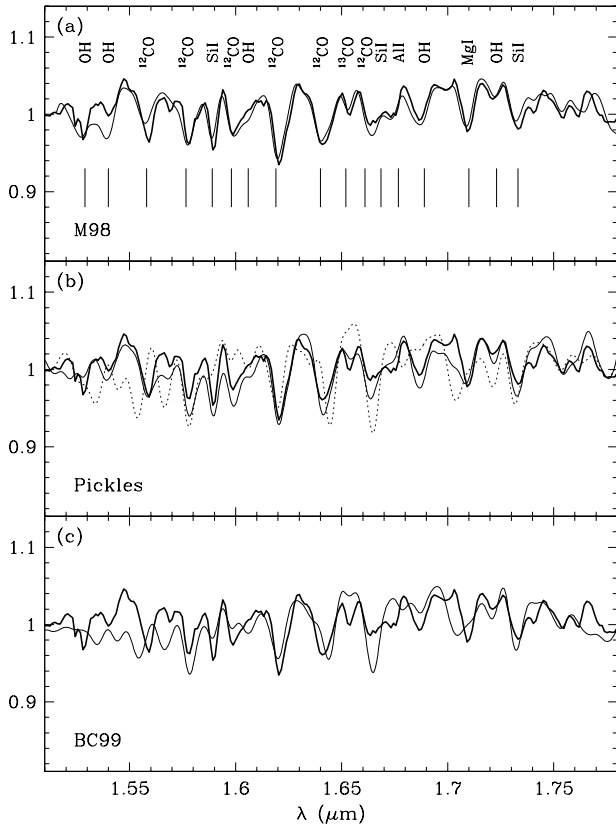


Figure 10. Line identifications and comparison of the observed H-band spectrum of the early-type galaxies (thick line) normalized to its continuum to several spectral libraries (thin lines) reduced to the same resolution. Panel (a): the galaxy spectrum is compared to a K5-giant star from the libraries by M98, showing a very good agreement. Panel (b): the spectra of a K5 (solid) and a MO giant (dotted) from Pickles (1998) are overlaid to the galaxy data. Even if the two stars are similar, their spectra in this library are very different. Panel (c): the SSP model from BC99 at 10 Gyr with empirical stellar libraries (see previous section and Figure 9) is compared to the data.

stars by their near-IR spectra (see references below). Usually two sets of lines are considered to derive both the spectral and the luminosity class, the first set depending both on temperature and gravity, while the second one on temperature only. The recipes used for star classification can also be applied to the observed galaxy spectra to derive indications on the the dominant stellar population.

We took into account two schemes of classification. They are both based on the CO(2,0) band head at $2.29 \mu\text{m}$ whose intensity depends both on temperature and luminosity and can be used to study the stellar populations in galaxies or in dusty regions (e.g., Armus et al., 1995; James & Seigar, 1999; Mobasher & James, 2000). The two methods use different thermometers: the first one, introduced by KH86 and refined by Ramirez et al. (1997), is based on the Equivalent Width (EW) of NaI $2.21 \mu\text{m}$ and CaI $2.26 \mu\text{m}$ which depend strongly on temperature but not on luminosity. In the second one, based on Origlia et al. (1993), the

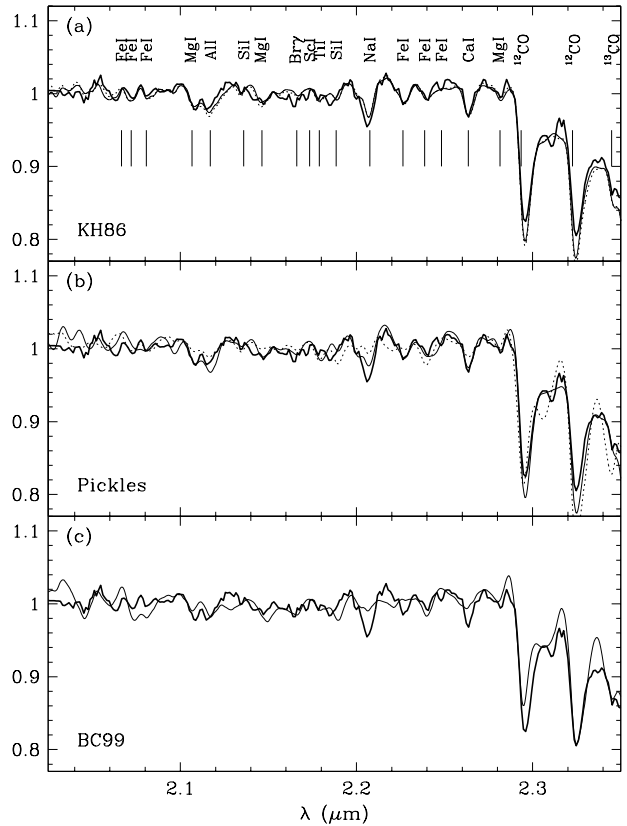


Figure 11. As the previous figure, but in the K band. The K5III star spectrum in panel (a) is from KH86.

temperature is measured by the ratio of the two features at 1.62 and $1.59 \mu\text{m}$. In both cases, the results for the galaxies are compared with those for the stars of known properties.

To apply these methods, we measured the EW of the lines with respect to a local continuum obtained by fitting a straight line to the "clear" parts of the spectrum. The spectral region used for both the line and the continuum are listed in Table 4. The same procedure was used to measure the EWs of the stars of the M98 and KH86. Because of the lower resolution of our spectra, our definitions are a little different from those by, for example, KH86 or Origlia et al. (1993), and the measured values of the EWs are consequently different. The errors on these quantities were estimated by taking into account both the noise of the spectra and the uncertainties in the continuum level. The latter contribution is usually the dominant one, especially in H where many features are present and it is difficult to define the continuum level. The results for the lines used in the classification are shown in Table 5 for the average ES spectra and in Table 6 for the individual galaxies not used for the templates. It should be noted that the error on the $1.62/1.59$ ratio shown in the table is smaller than the error on each single line because the same continuum fit is used: the uncertainties on the continuum level strongly affect the measure of the EW of each line, but partially cancel out from their ratio.

In Figure 12 we present the classification based on the

Table 4. Feature definition

Feature	Line (μm)	Continuum (μm)
1.59	1.586-1.594	1.572-1.574, 1.608-1.613 1.628-1.633
1.62	1.616-1.629	1.572-1.574, 1.608-1.613 1.628-1.633
NaI	2.204-2.211	2.191-2.197, 2.213-2.217
CaI	2.258-2.269	2.245-2.256, 2.270-2.272
$^{12}\text{CO}(2,0)$	2.289-2.302	2.270-2.272, 2.275-2.278 2.282-2.286, 2.288-2.289

Table 5. Value of the EW (\AA) measured on the templates, and their errors

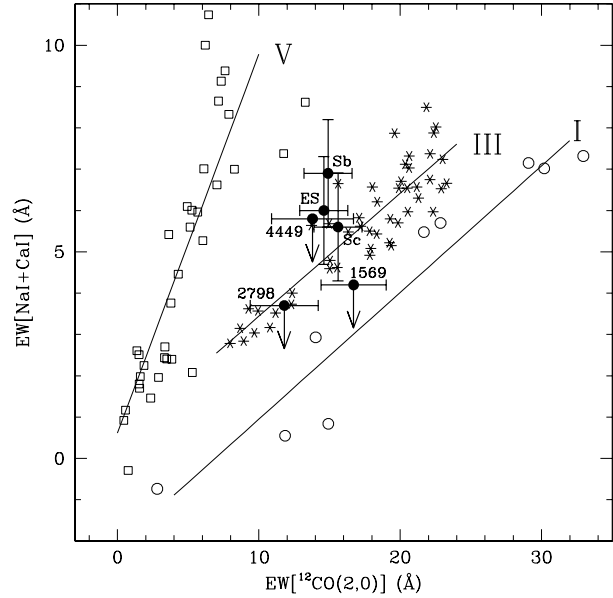
Feature	E+S0+Sa	Sb	Sc
1.59	3.9 (0.8)	3.7 (0.9)	3.3 (0.9)
1.62	6.0 (0.7)	5.6 (0.8)	5.7 (0.8)
1.59/1.62	1.5 (0.1)	1.5 (0.2)	1.7 (0.2)
$^{12}\text{CO}(2,0)$	14.6 (1.7)	15.8 (1.7)	15.6 (1.7)
CaI	2.6 (1.1)	2.7 (1.1)	2.2 (1.1)
NaI	3.4 (0.7)	4.2 (0.7)	3.4 (0.7)

features in the K band studied by KH86 and Ramirez et al. (1997). This figure differs from both works because the feature definition is different (because of the lower resolution) and because we don't take into account the EW of Br γ which cannot be reliably measured. As expected, the results show that in all the cases the main role is played by class III stars, possibly with some contribution from dwarf stars. With the present data it does not seem possible to measure this contribution and therefore constraint the ratio between dwarf and giant stars, but this could be done with higher resolution observations. The spectra of the active galaxies (see Figure 4) are too noisy to measure the EWs of NaI and CaI, and only upper limits can be derived. As shown in Figure 12, these upper limits put two of these galaxies in the region between class I and class III stars, suggesting that the contribution supergiants might be important in these galaxies.

In Figure 13 we apply the second method based on the CO feature at $2.29\mu\text{m}$ and on the ratio of the 1.59 and $1.62\mu\text{m}$ in the H band. This method is based on the work by Origlia et al (1993) who showed that this ratio can be used as a thermometer in case of giants and supergiants stars. Also in this case the line ratio is consistent with the class

Table 6. Value of the EW (\AA) measured for the active galaxies, and their errors

	NGC2798	NGC1569	NGC4449
$^{12}\text{CO}(2,0)$	11.8 (2.4)	16.7 (2.3)	13.8 (2.9)
NaI+CaI	< 3.7	< 4.2	< 5.8


Figure 12. The sum of the EWs of NaI ($2.21\mu\text{m}$) and CaI ($2.26\mu\text{m}$) is plotted versus the EW of the $^{12}\text{CO}(2,0)$ band at $2.29\mu\text{m}$. The solid dots with the error bars are our galaxies, while dwarf, giant and supergiant stars are plotted as empty squares, stars and empty circle respectively (see text for references). The lines are linear fit to the stellar data, with the indication of the luminosity class.

III stars.

A discussion about the metallicity of ellipticals and early spirals is beyond the scope of this paper. Detail discussions about the information of metallicity and element ratios based on optical data can be found, for example, in Worthey (1998) and Trager et al. (2000). Origlia et al. (1997) have shown that moderate-resolution near-IR spectra can also be used to measure the metallicity of the systems. Their recipe is based on the $1.62\mu\text{m}$ feature which is shown to depend on the metallicity index $[\text{Fe}/\text{H}]$ and, more weakly, on the carbon depletion factor $[\text{C}/\text{Fe}]$. It also depends on the microturbulent velocity ξ of the dominant stellar populations because this quantity influences the strength of the saturated molecular lines. By observing globular clusters of known metallicity, Origlia et al. (1997) show that this metallicity scale gives errors smaller than 0.3 dex. These authors have also observed a limited number of elliptical galaxies. The few metallicity estimates published for these objects are based on the Mg2 index (see, for example, Davies et al., 1987) and on the Mg2-metallicity calibration by Casuso et al. (1996). While the Mg2-derived value of $[\text{Fe}/\text{H}]$ of the observed galaxies was solar or slightly supersolar, between +0.08 and +0.21, the values based on the near-IR lines turned out to be subsolar, between -0.28 and -0.46. This can be explained either by the presence of a corresponding Magnesium enhancement of about $[\text{Mg}/\text{Fe}] \simeq 0.5$, as proposed by several authors (see Origlia et al., 1997 for details), or by an anticorrelation between $[\text{C}/\text{Fe}]$ and $[\text{Fe}/\text{H}]$, the more metallic objects being more carbon depleted, as observed in the globular clusters.

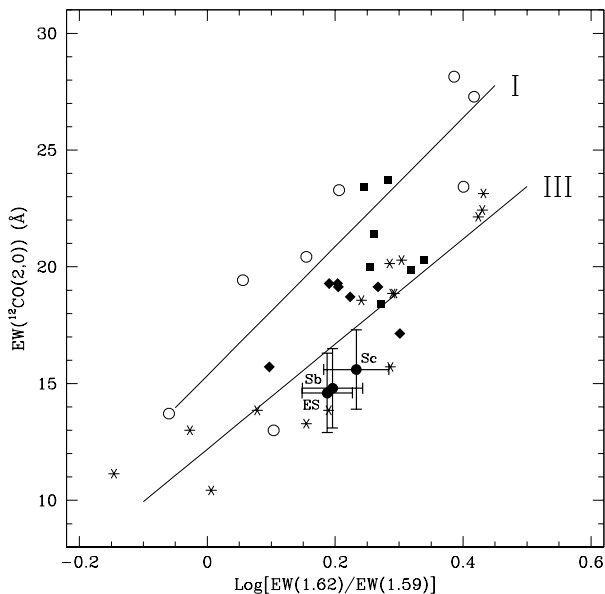


Figure 13. EW of the $^{12}\text{CO}(2,0)$ feature at $2.29\mu\text{m}$ vs. the ratio $\text{EW}(1.62)/\text{EW}(1.59)$. Giants and supergiants stars (see text for references) are plotted by empty circles and stars respectively. The galaxies observed by Origlia et al. (1993) are plotted by solid diamonds if quiescent ellipticals and spirals, and solid squares if H III galaxies. Solid circles with error bars are the galaxies of this study. The lines are the linear fit to the stellar data.

More recently, several authors (Trager et al., 2000; Worthey, 1998) would rather explain the non-solar $[\text{Mg}/\text{Fe}]$ with a depletion of the iron-peak elements.

Despite the large uncertainties on the right value of $[\text{C}/\text{Fe}]$ and on the resulting metallicity, we have applied this method to our early-type galaxies (ES spectrum, see table 5). By iteratively solving the eq. 2 by Origlia et al. (1997) we obtain a mean microturbulent velocity ξ of about 3.1 km/sec , in agreement with the values between 2.3 and 3.0 in Origlia et al. (1997). By using the 'standard' value of $[\text{C}/\text{Fe}] = -0.3$ suggested by these authors and derived for the Magellanic Clouds clusters by Oliva & Origlia (1998), the metallicity derived from their eq. 1b is $[\text{Fe}/\text{H}] \simeq -0.20$, reducing to $[\text{Fe}/\text{H}] \simeq -0.4$ for $[\text{C}/\text{Fe}] = 0.0$. The error on this quantity is difficult to estimate and is probably dominated by the uncertainties on $[\text{C}/\text{Fe}]$, but this result can be used as an indication of sub-solar abundance of iron in the early-type galaxies.

9 SUMMARY

The near-IR spectra of 28 nearby galaxies were used to define the “average” J, H and K spectra of normal galaxies along the Hubble diagram between E and Sc. The target objects and the aperture were chosen to be similar to those by K96 in order to merge the two data sets and obtain self-consistent spectra between 0.1 and $2.4 \mu\text{m}$. The average effective colours of the galaxies of the various classes were used

to calibrate the final spectra. The overall precision is about 2%.

The spectra were used to compute the k-corrections in the near-IR bands and to check the predictions of several spectrophotometric models of galaxy evolution. We find that most model can accurately reproduce the observed continuum shape of the elliptical galaxies, if solar metallicities are assumed. In this case the derived SSP ages at above 8 Gyr. Nevertheless, large differences are found between the models, for example in terms of the derived age of the dominant stellar population.

On the other hand, larger discrepancies are found between the observed spectral features and the predictions of the models. We note that the spectra of cool giant stars from some accurate libraries (as KH86 and M98) can reproduce the observed features in great detail, and conclude that the disagreement is probably due to the stellar libraries used in the models.

The spectral features are also used to study the stellar populations by using several stellar classification recipes based on near-IR absorption lines, some of them applied to galaxies for the first time. The dominant contribution to the near-IR emission of all the galaxies between E and Sc is confirmed to be due to giant stars of spectral type about K5, with solar or slightly subsolar metallicity.

The final spectra for each galaxy type, the relative k-corrections (both in the Bessel & Brett and in the CIT systems) and the profiles of the used filters can be downloaded from the web site www.arcetri.astro.it/~filippo/spectra. In some cases it could be useful to simulate the spectra of galaxies with colours different from those in Table 2, for example to reproduce individual galaxies or match total colours. In the same web site it is possible to define a new set of colours, compute the corresponding spectra and download the results.

10 ACKNOWLEDGMENTS

We are grateful to Tino Oliva, Livia Origlia and Valentin Ivanov, for enlightening discussions about near-IR spectra and stellar classification, and to Stephan Charlot and Gustavo Bruzual for having provided us a recent version of their model. We are also grateful to the TIRGO staff for the support during the observations. LP acknowledges a partial support from the ASI grant ASI-ARS99-44.

REFERENCES

- Aaronson, M., 1978, ApJ 221, L103
- Ali, B., Carr, J. S., DePoy, D. L., Frogel, J. A., & Sellgren, K., 1995, AJ 110, 2415
- Armus, L., Neugebauer, G., Soifer, B.T., & Matthews, K., 1995, AJ 110, 2610
- Barbaro G., Poggianti B.M., 1997, A&A, 324, 490
- Bessell, M. S., & Brett, J. M., 1988, PASP 100 1134
- Bessell, M. S., Brett, J. M., Sholz, M. & Wood, P. R., 1991, A&AS, 89, 335
- Bressan, A., Fagotto, F., Bertelli, G. & Chiosi, C. 1993, A&ASS, 100, 647
- Bruzual, A.G., & Charlot, S., 1993, ApJ 405, 538

- Buta, R., Mitra, S., De Vaucouleurs, G., & Corwin, H.G., 1994, AJ 107, 118
- Buta, R., & Williams K. L., 1995b, AJ 109, 543
- Buta, R., Corwin, H.G. Jr., de Vaucouleurs, G., de Vaucouleurs A. & G. Longo, 1995a, AJ, 109, 517
- Cardelli, J.A., Clayton, G.C. & Mathis, J.S., 1989, ApJ, 345, 245
- Casuso, E., Vazdekis, A., Peletier, R.F., & Beckman, J.E., 1996, ApJ 458, 533
- Charlot, S., Worthey, G., & Bressan, A., 1996, ApJ 457, 625
- Coleman, G. D., Wu, C.-C., & Weedman, D. W., 1980, ApJS 43, 393
- Cowie, L. L., Gardner, J. P., Hu, E. M., Songaila, A., Hodapp, K.-W., & Wainscoat, R. J., 1994, ApJ 434, 114
- Dallier R., Boisson C., & Joly M., 1997, A&ASS, 116, 239
- Davies, R.L., Burstein, D., Dressler, A., Faber, S.M., Lynden-Bell, D., Terlevich, R.J., & Wegner, G., 1987, ApJS 64, 581
- Fioc, M., Rocca-Volmerange, B., 1997, A&A 326, 950
- Fioc, M., & Rocca-Volmerange, B., 1999, A&A, 351, 869
- Frei, Z., & Gunn, J. E., 1994, AJ 108, 1476
- Frogel, J.A., Persson, S.E., Aaronson, M., & Matthews, K., 1978, ApJ 220, 75
- Giovanardi, C., & Hunt, L. H., (1988), AJ 95, 408
- Glass, I.S., 1984, MNRAS 211, 461
- Glazebrook, K., Peacock, J. A., Miller, L., & Collins, C. A., 1995, MNRAS 275, 169
- Glazebrook, K., Offer, A. R., & Deeley, K., 1998, ApJ 492, 98
- Green, E. M., Demarque, P. & King, C. R., 1987, The Revised Yale Isochronoses and Luminosity Functions, New Haven: Yale University Observatory
- Griensmith, D., Hyland, A.R., & Jones, T.J., 1982, AJ 87, 1106
- Goudfrooij, P., 1994, PhD thesis, Univ.....
- James, P. A., & Seigar, M. S., 1999, A&A 350, 791
- de Jong, R.S., & van der Kruit, P.C., 1994, A&AS 106, 451
- Kennicutt, R. C. Jr., & Kent, S. M., 1983, ApJ, 88, 1094
- Kennicutt, R.C., 1992, ApJ 388, 310
- Kennicutt, R.C., 1992, ApJS 79, 255
- Kinney, A.L., Calzetti, D., Bohlin, R.C., McQuade, K., Storchi-Bergmann, T., & Schmitt, H.R., 1996, ApJ 467, 38 (K96)
- Klienmann, S.G., & Hall, D.N.B., 1986, ApJS 62, 501
- Kurucz R., 1993, AAS CD-ROM series n.13
- Ivanov, V. D., Rieke, M. J., Alonso-Herrero, A., Engelbracht, C. W., Luhman, K. L. & Rieke, G. H. 1999, American Astronomical Society Meeting, 195, 113603
- Lançon, A., Mouhcine, M., Fioc, M., & Silva, D., 1999, A&A, 344, L21
- Lançon, A., & Rocca-Volmerange, B., 1992, A&AS 96, 593
- Lejeune, th., Cuisinier, F., & Buser, R., (1997) A&AS 125, 229
- Livingston, W., & Wallace, L., 1991, An Atlas of the solar spectrum in the infrared from 1850 to 9000 cm^{-1} , National Solar Observatory Technical Report 91-001
- Loveday, J. (2000) AAS 195, 557
- Maiolino, R., Rieke, G.H., & Rieke, M.J., 1996, AJ 111, 537
- Maraston, C., 1998, MNRAS 300, 872
- Meyer, M.R., Edwards, S., Hinkle, K., & Strom, S.E. 1998, ApJ 508, 397
- Mobasher, B., & James, P.A., 2000, MNRAS, 316, 507
- Mouhcine, M., & Lançon, A., 1999, in "Spectrophotometric dating of stars and galaxies", Annapolis, Maryland (U.S.A.), eds. I. Hubeny, S. Heap, & R. Cornett, PASP Conf. Ser. (astro-ph/9906149)
- Oliva, E., Origlia, L., Kotilainen, J. K. & Moorwood, A. F. M. 1995, A&A, 301, 55
- Oliva, E. & Origlia, L. 1998, A&A, 332, 46
- Origlia, L., Ferraro, F. R., Fusi Pecci, F. & Oliva, E. 1997, A&A, 321, 859
- Origlia, L., Moorwood, A. F. M. & Oliva, E. 1993, A&A, 280, 536
- Origlia, L., Goldader, J. D., Leitherer, C., Schaerer, D. & Oliva, E. 1999, ApJ, 514, 96
- Origlia, L. & Oliva, E. 2000, A&A, 357, 61
- Peebles, P. J. E., 1993, "Principles of physical cosmology", Princeton Series in Physics
- Pence, W., 1976, ApJ 203, 39
- Persson, S.E., Frogel, J.A., & Aaronson, M., 1979, ApJS 39, 61
- Pickles, A.J., 1998, PASP 110, 863
- Poggianti, B. M., 1997, A&AS, 122, 399
- Prugniel, Ph, & Hèraudeau, Ph., 1998, A&AS 128, 299
- Ramirez, S.V. DePoy, D.L., Frogel, J.A., Sellgren, K., & Blum, R.D. 1997, AJ 113, 1411
- Rana, N.C., & Basu, S., 1992, A&A 265, 499
- Rocca-Volmerange, B. & Guiderdoni, B., 1988, A&AS 75, 93
- Szokoly, G. P., Subbarao, M. U., Connolly, A. J. & Mobasher, B. 1998, ApJ, 492, 452
- Tantalo, R., Chiosi, C., Bressan, A., & Fagotto, F., 1996, A&A 311, 361
- Trager, S. C., Faber, S. M., Worthey, G., & Gonzales, J.J., 2000, AJ 119, 1645
- VandenBerg, D. A., & Laskarides, P. G., 1987, ApJS, 64, 103
- Vanzi, L., & Rieke, G.H., 1997, ApJ 479, 694
- Vanzi, L., et al. 1997, A&AS, 124, 573
- de Vaucouleurs G., de Vaucouleurs A., Corwin H.G., Buta R.J., Paturel G., Fouque P., 1991, "Third Reference Catalogue of Bright Galaxies (RC3)" Springer-Verlag: New York
- Wallace L., & Hinkle K., 1996, ApJS, 107, 312
- Wallace L., & Hinkle K., 1997, ApJS, 111, 445
- Wallace L., Meyer, M.R., Hinkle, K., & Edwards, S., 2000, ApJ, 535, 352
- Worthey, G., 1994, ApJS 95, 107
- Worthey, G., 1998, PASP 110, 888
- Yee, H. K. C., 1998, in "Birth of Galaxies", (Paris, Edition Frontieres), eds. B.Guiderdoni, F.Bouchet, T.X.Thuan & J.T.T.Van (astro-ph/9809347)